

Transients Caused by Switching of 420 kV Three-Phase Variable Shunt Reactor

B. Filipović-Grčić, A. Župan, I. Uglešić, D. Mihalic, D. Filipović-Grčić

Abstract--This paper describes transients caused by uncontrolled and controlled switching of three-phase 420 kV variable shunt reactor (VSR). The model for the analysis of the transients caused by switching of VSR was developed in EMTP-RV software which includes dynamic electric arc in SF₆ circuit breaker and the model of substation equipment. Inrush currents due to VSR energization and overvoltages due to de-energization were determined at tap positions corresponding to lowest 80 MVar and highest 150 MVar reactive power. Based on the calculation results, mitigation measures and operating switching strategy of VSR were proposed.

Keywords: variable shunt reactor, SF₆ circuit breaker, controlled switching, inrush current, electric arc model, EMTP-RV simulations.

I. INTRODUCTION

THE function of shunt reactors in transmission networks is to consume the excessive reactive power generated by overhead lines under low-load conditions, and thereby stabilize the system voltage. They are quite often switched on and off on a daily basis, following the load situation in the system. Instead of having two or more shunt reactors with fixed power ratings, a single variable shunt reactor (VSR) could be used for compensation of reactive power.

The actual magnitude of the inrush current due to VSR energization is quite dependent on the range of linearity of the VSR core and on the time instant of circuit breaker pole operation. Switching operations at unfavorable instants can cause inrush currents that may reach high magnitudes and have long time constants. In case when VSRs have solidly grounded neutral, unsymmetrical currents cause zero-sequence current flow which can activate zero-sequence current relays. This may cause difficulties such as unwanted operation of the overcurrent relay protection [1].

De-energization of the VSR can impose a severe duty on both the shunt reactor and its circuit breaker due to current chopping that occurs when interrupting small inductive currents. The switching overvoltages can be dangerous for the equipment if the peak value exceeds the rated switching impulse withstand voltage of the VSR. However, overvoltages resulting from the de-energization are unlikely to cause insulation breakdown of VSRs as they are protected by surge arresters connected to their terminals. The severity of the switching duty increases when single or multiple reignitions occur. Such voltage breakdowns create steep transient overvoltages on VSR with the front time ranging from less than one microsecond to several microseconds and may be unevenly distributed across the VSR winding. So these steep fronted transient voltages are stressing the entrance turns in particular with high inter-turn overvoltages. Therefore some mitigation measures should be considered to reduce the chopping overvoltages and the risk of reignition of the circuit breakers.

Uncontrolled switching of shunt reactors, shunt capacitors and transmission lines may cause severe transients such as high overvoltages or high inrush currents [2]. Conventional countermeasures such as pre-insertion resistors, damping reactors or surge arresters can be used to limit the switching transients. In addition, system and equipment insulation can be upgraded to withstand the dielectric stresses. These methods, however, may be inefficient, unreliable or expensive, and do not treat the root of the problem [3].

Controlled switching is a method for eliminating harmful transients via time controlled switching operations. Closing or opening commands to the circuit breaker are delayed in such a way that switching occurs at the optimum time instant related to the voltage phase angle. Controlled switching has become an economical substitute for a closing resistor and is commonly used to reduce switching surges. The number of installations using controlled switching has increased rapidly due to satisfactory service performance since the late 1990s [4], [5]. Currently, it is often specified for shunt capacitor and shunt reactor banks because it can provide several economic benefits such as the elimination of closing resistors and the extension of a circuit breaker nozzle and contact maintenance interval. It also provides various technical benefits such as improved power quality and the suppression of transients in transmission and distribution systems [6].

This paper describes transients caused by switching of three-phase 420 kV VSR. Inrush currents due to VSR energization and overvoltages due to de-energization were

This work has been supported in part by the Croatian Science Foundation under the project "Development of advanced high voltage systems by application of new information and communication technologies" (DAHVAT).

B. Filipović-Grčić and I. Uglešić are with the University of Zagreb, Faculty of Electrical Engineering and Computing, Unska 3, 10000 Zagreb, Croatia (e-mail: bozidar.filipovic-grcic@fer.hr, ivo.uglesic@fer.hr).

A. Župan and D. Mihalic are with the Croatian Transmission System Operator Ltd., Kupaska 4, 10000 Zagreb, Croatia (e-mail: alan.zupan@hops.hr, dragutin.mihalic@hops.hr).

D. Filipović-Grčić is with the KONČAR – Electrical Engineering Institute, 10000 Zagreb, Croatia (email: dfilipovic@koncar-institut.hr).

analyzed. For this purpose, a model of VSR, substation equipment and electric arc in SF₆ circuit breaker was developed in EMTP-RV software.

II. MODEL IN EMTP-RV

VSR considered in this paper has 29 tap positions, and the tap-changing order is in opposite direction, i.e. it starts from tap position 29 (lowest amount of 80 MVar consumption) and the final position is 1 (highest amount of 150 MVar consumption). The VSR lowers the voltage by tapping from tap position 29 to tap position 1. VSR manufacturer data are shown in Table I.

TABLE I VSR DATA

Rated voltage	420 kV	
Rated frequency	50 Hz	
Reactive power	150 MVar (tap position 1)	80 MVar (tap position 29)
Rated current	206 A	110 A
Core type	Five limb	
Total losses (at 420 kV)	232 kW	145 kW
Zero sequence impedance	1.2 kΩ per phase	2.2 kΩ per phase
Capacitance of winding to ground	3.8 nF per phase	

Fig. 1 shows the change of VSR reactive power, current and impedance with respect to tap position.

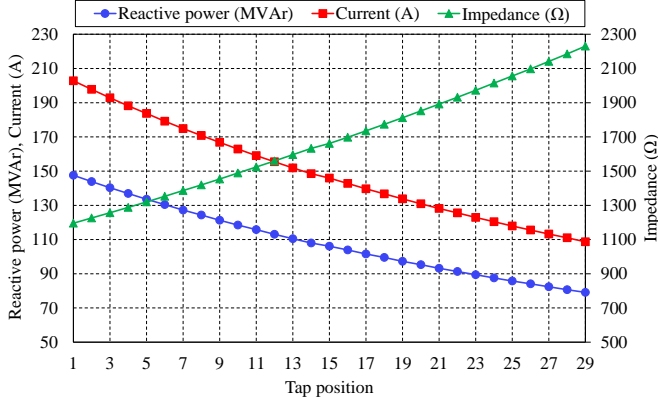


Fig. 1. VSR power, current and impedance versus tap position

VSR switching transients were calculated only in case of lowest (80 MVar) and highest (150 MVar) reactive power. The calculation of inrush currents requires an adequate modeling of the reactor nonlinear flux-current curve. The nonlinearity is caused by the magnetizing characteristics of the VSR iron core. Recorded RMS voltage-current curves obtained from manufacturer were converted into instantaneous flux-current saturation curves (Fig. 2) which were used in the nonlinear inductance model in EMTP-RV [7] and approximated with two segments (linear area A-B, below knee of the saturation curve and saturation area B-C).

Each phase of a three phase VSR was modeled as a nonlinear inductance with serially connected resistance $R_{Cu}=1.36 \Omega$, representing copper losses and parallel connected

$R_{Fe}=3.04 \text{ k}\Omega$, representing iron losses. Magnetic coupling among the three star connected phases was represented with zero-sequence inductance $L_0=3.7 \text{ H}$ which provides a path for the zero sequence current [8].

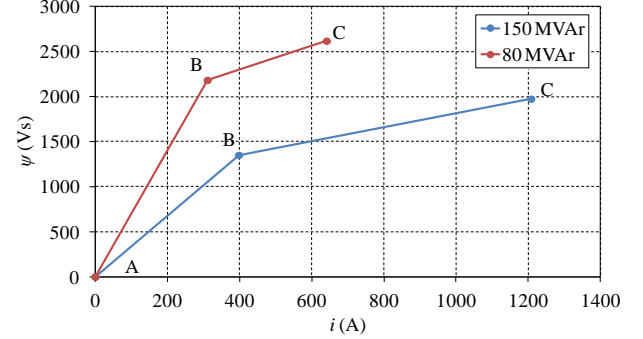


Fig. 2. Instantaneous flux-current saturation curve of VSR

VSR model in EMTP-RV is shown in Fig. 3.

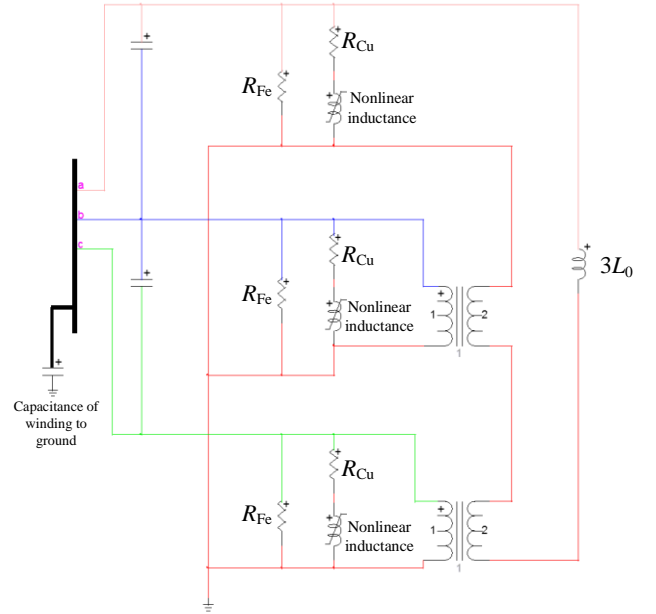


Fig. 3. VSR model in EMTP-RV

The equivalent 420 kV network was represented with positive ($R_1=1.1 \Omega$, $L_1=47.13 \text{ mH}$) and zero ($R_0=3.14 \Omega$, $L_0=64.87 \text{ mH}$) sequence impedances, determined from single-phase and three-phase short circuit currents.

The equipment in high voltage substation was represented by surge capacitances [9], whereas busbars and connecting leads by a frequency dependent line model. MO surge arresters in VSR bay with rated voltage $U_r=330 \text{ kV}$ were modeled with nonlinear $U-I$ characteristic with respect to switching overvoltages.

SF₆ circuit breaker with two breaking chambers was represented by Schwarz-Avdonin electric arc model [10], [11] and grading capacitors of 500 pF connected in parallel to breaking chambers. EMTP-RV model shown in Fig. 4 consists of equivalent 420 kV network, main busbars, SF₆ circuit breaker and equipment in VSR bay.

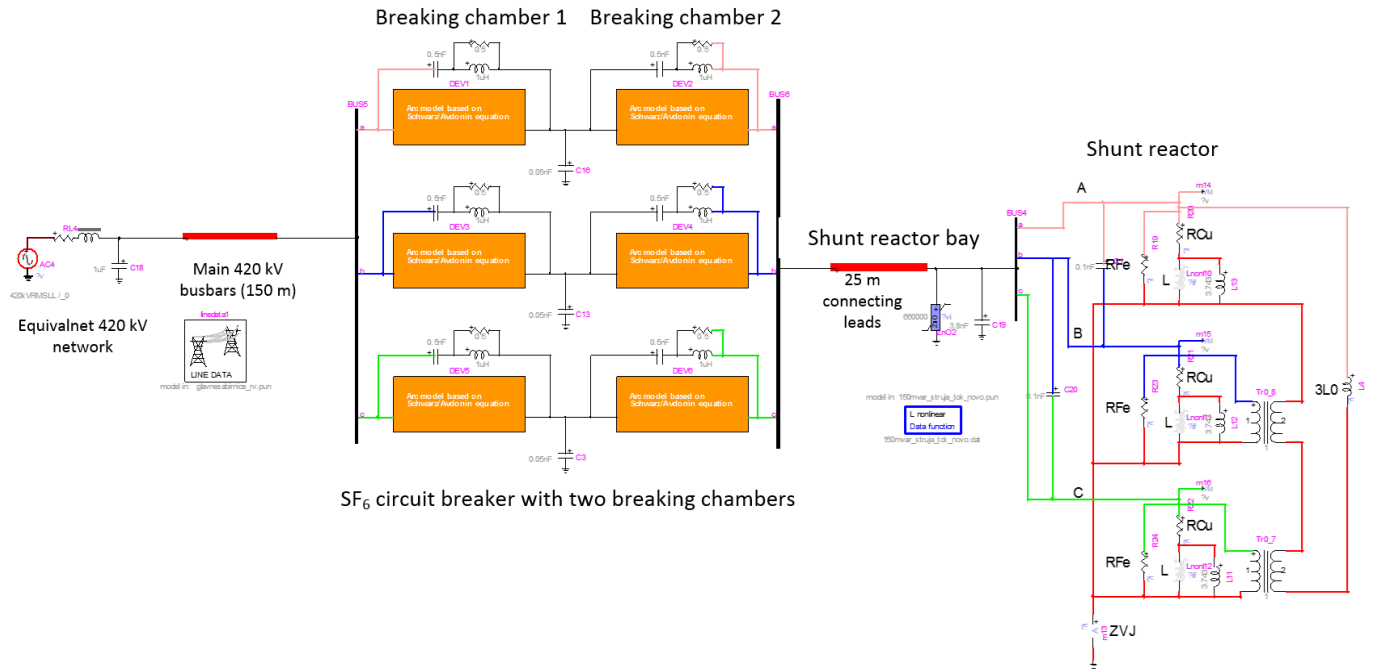


Fig. 4. EMTP-RV model of VSR, equipment in substation and equivalent network

III. UNCONTROLLED ENERGIZATION OF VSR

The following instants of circuit breaker pole closing were considered: $t_A=15$ ms, $t_B=13$ ms and $t_C=17$ ms (Fig.5). Simulations were carried out in case of VSR lowest (80 MVar) and highest (150 MVar) reactive power.

A. Tap position 1: reactive power 150 MVar

Figs. 5 and 6 show calculated VSR voltages and currents, respectively. The highest inrush current occurs at an instant near the voltage zero-crossing in phase A, since it results with the maximum DC component of current.

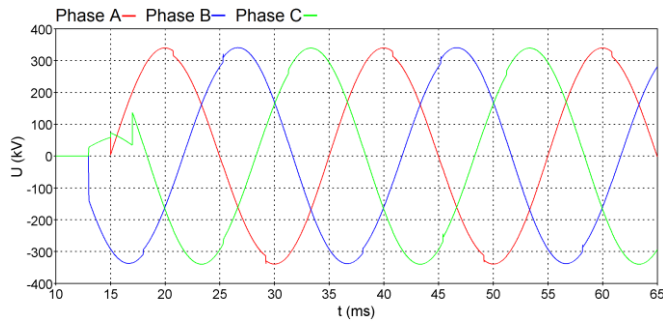


Fig. 5. VSR voltages

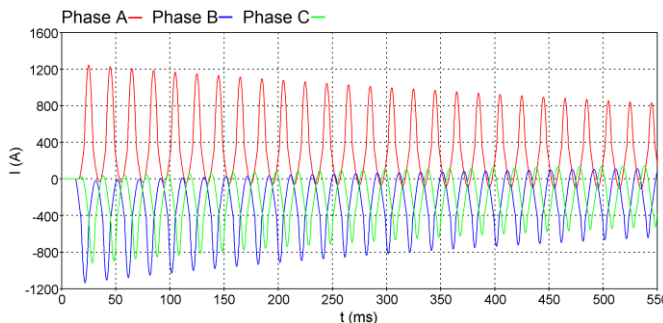


Fig. 6. VSR currents: $I_{Amax}=1245.2$ A (4.27 p.u.)

The conducted simulation showed that transient inrush current with amplitude of 4.27 p.u. and high DC component lasted for 3.2 seconds (Fig. 7). This could cause difficulties such as unwanted operation of the overcurrent relay protection.

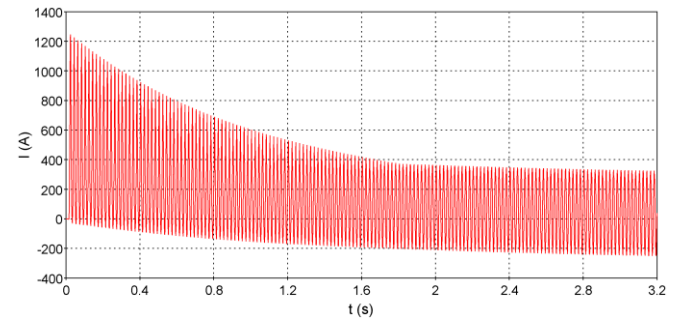


Fig. 7. VSR current in phase A

Zero-sequence current occurred in case of uncontrolled reactor energization (Fig. 8) as a consequence of asymmetry. This may cause the false operation of relay protection used for detecting single phase-to-ground faults.

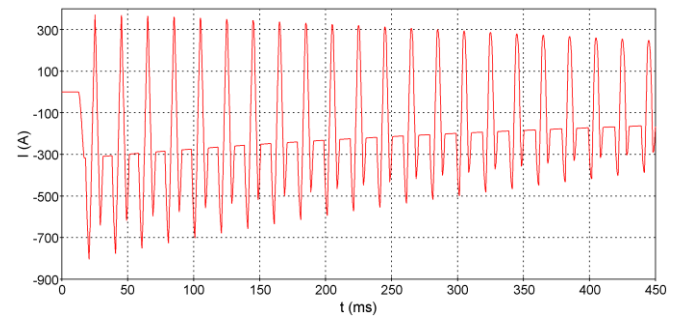


Fig. 8. VSR zero-sequence current, $I_{max}=-806$ A (2.76 p.u.)

B. Tap position 29: reactive power 80 MVar

Figs. 9-12 show calculation results. The conducted simulation showed that transient inrush current with amplitude of 2.16 p.u. and high DC component lasted for 4 seconds (Fig. 11). Inrush currents and zero-sequence currents were significantly lower in this case compared to 150 MVar (Fig. 12).

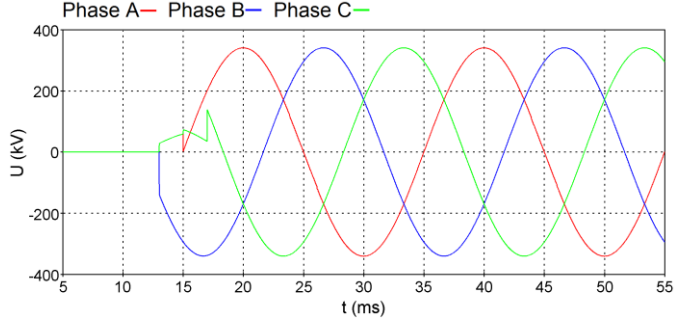


Fig. 9. VSR voltages

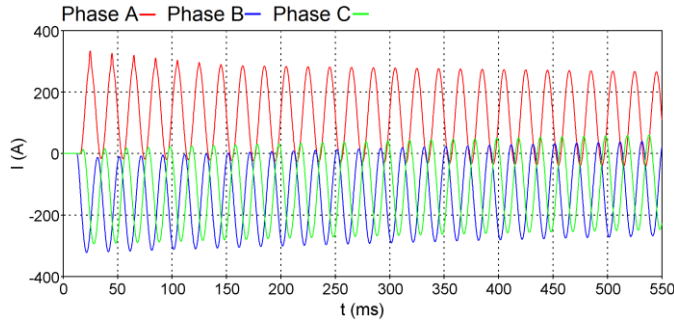


Fig. 10. VSR currents: $I_{Amax} = 334.2$ A (2.16 p.u.)

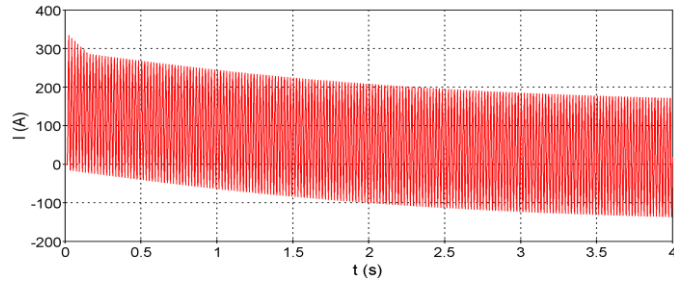


Fig. 11. VSR current in phase A

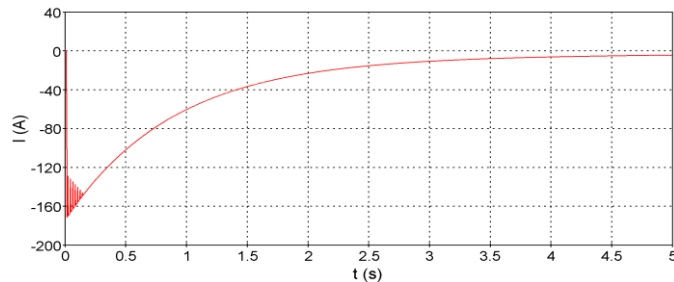


Fig. 12. VSR zero-sequence current, $I_{max} = -171.5$ A (1.11 p.u.)

IV. CONTROLLED ENERGIZATION OF VSR

Controlled energization at optimum instants of circuit breaker poles closing at peak voltages: $t_A = 10$ ms, $t_B = 6.66$ ms and $t_C = 13.33$ ms (Fig. 13) were analyzed.

A. Tap position 1: reactive power 150 MVar

Figs. 13 and 14 show VSR voltages and currents.

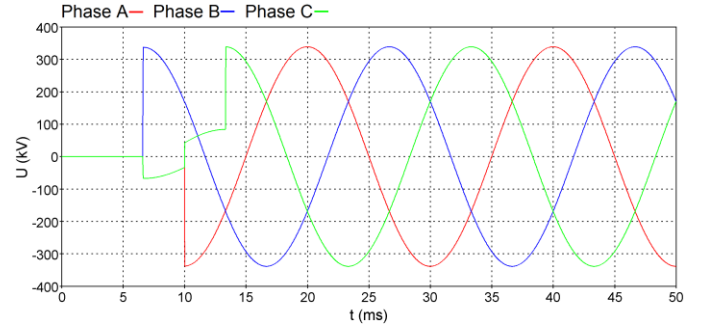


Fig. 13. VSR voltages

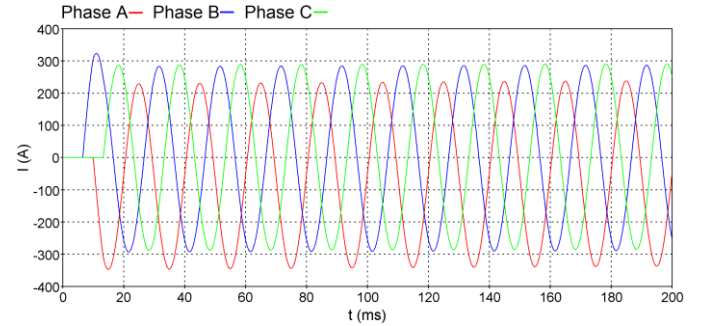


Fig. 14. VSR currents, $I_{Amax} = -347.8$ A (1.19 p.u.)

The current in phase A (Fig. 14) was slightly higher than in the other two phases, due to the appearance of the DC component, which was caused by initial magnetic flux in the core limb at the moment of energization. This initial magnetic flux is a part of a magnetic flux from the phase B, which was firstly switched on (Fig. 15). The final distribution of the magnetic flux in the reactor core is shown in Fig. 15.

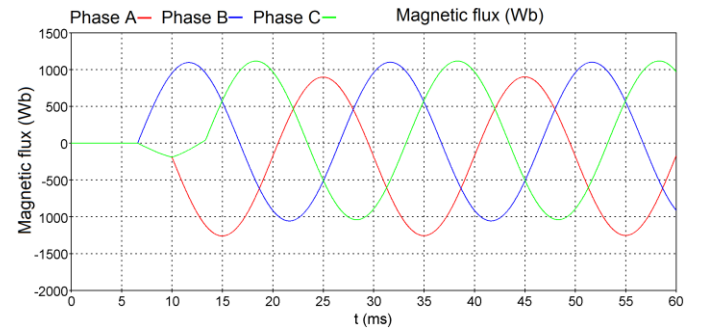


Fig. 15. Magnetic flux in case of VSR controlled energization

Due to the air gaps (Fig. 16) utilized in VSR core there were no severe saturation effects [12]. VSR is designed to combine the highest possible inductive power with compact size. For this purpose, iron-cored reactance coils with air gaps are used. The iron core conducts and concentrates the magnetic flux produced by the winding, which has to bridge the air gap. Due to the large difference between the permeability of magnetic sheet steel and oil, it is sufficient to use the magnetic resistance of the air gap for the series

connection of the iron and air path. The air gaps reduce inductance and increase the power output of this configuration. The conducted simulation showed that amplitudes and DC components of inrush current (Fig. 17) and zero-sequence current (Fig. 18) were significantly lower in case of controlled switching.

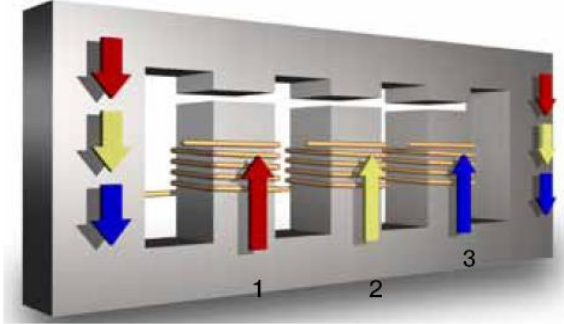


Fig. 16. The distribution of the magnetic flux in the five limb core of VSR - phase A (1), B (2) and C (3)

As a consequence, successfully controlled switching reduces the mechanical and electromagnetic stresses of the high voltage equipment and also prevents the unwanted operation of relay protection.

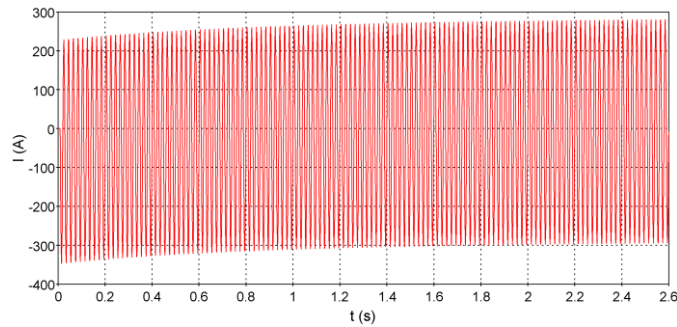


Fig. 17. VSR current in phase A

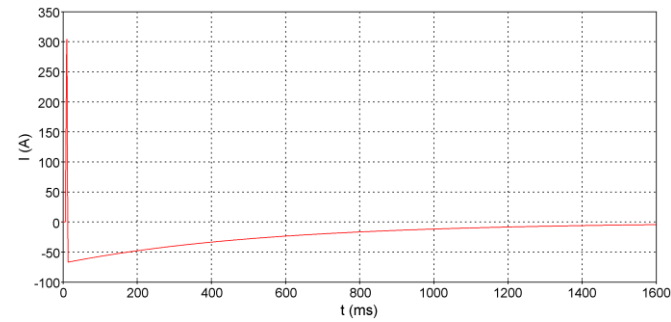


Fig. 18. VSR zero-sequence current

B. Tap position 29: reactive power 80 MVar

Figs. 19-22 show calculation results in case of 80 MVar. Controlled switching reduced inrush current and zero-sequence currents, which were lower in case of reactive power 80 MVar compared to 150 MVar.

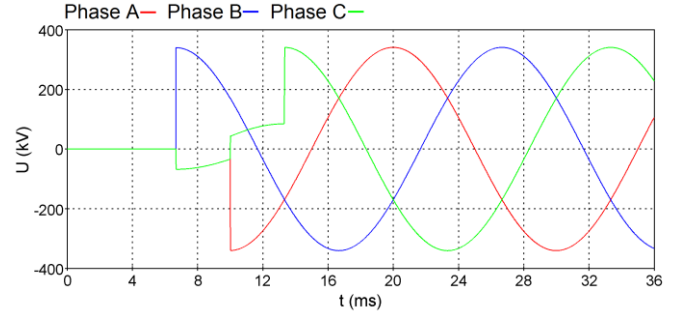


Fig. 19. VSR voltages

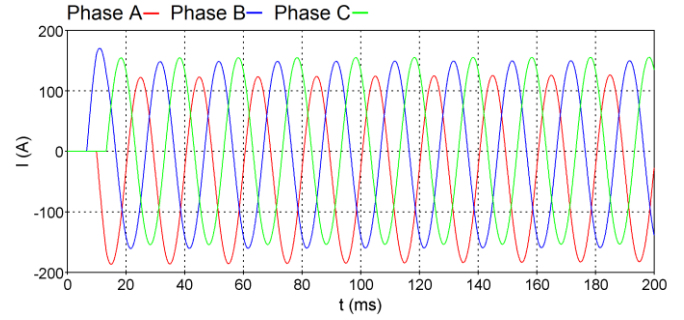


Fig. 20. VSR currents, $I_{Amax} = -187.0$ A (1.21 p.u.)

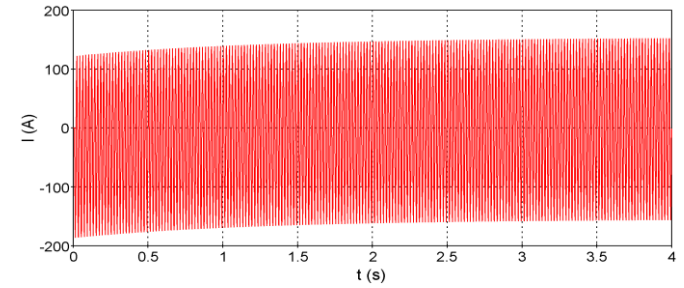


Fig. 21. VSR current in phase A

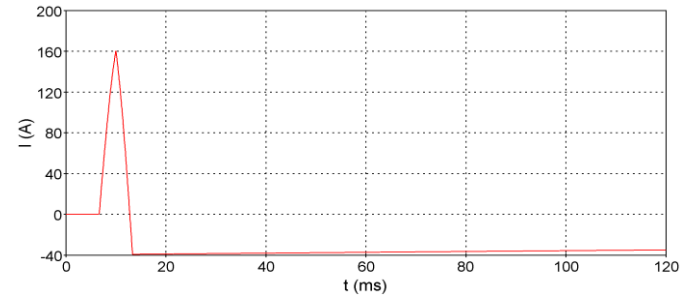


Fig. 22. VSR zero-sequence current, $I_{Zmax} = 160.4$ A (1.04 p.u.)

V. DE-ENERGIZATION OF VSR

Fig. 23 shows circuit breaker currents in case of 80 MVar de-energization and Fig. 24 shows current chopping in phase C. For small inductive currents, the cooling capacity of the circuit breaker dimensioned for the short-circuit current is much higher in relation to the energy dissipated in the electric arc. This led to arc instability and an oscillating phenomena shown in Fig. 24 occurred.

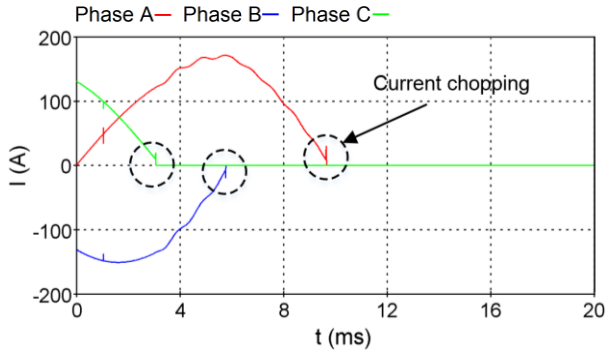


Fig. 23. Circuit breaker currents during the VSR de-energization

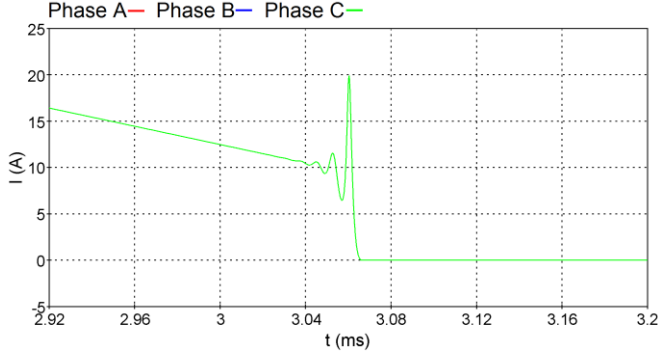


Fig. 24. Current chopping in phase C

During this high frequency oscillation, current passed through zero value and the circuit breaker interrupted the current before its natural zero-crossing at the 50 Hz frequency. This phenomenon was followed by a transient overvoltage mainly due to the oscillatory state which was set up on the VSR side. Tables II and III show calculated overvoltages on VSR and transient recovery voltages (TRV) on circuit breaker in case with installed surge arresters.

TABLE II CALCULATION RESULTS IN CASE OF 80 MVAR

Phase	Overvoltages on VSR U_{max} (kV)	TRV on circuit breaker U_{max} (kV)		
		Breaking chamber 1	Breaking chamber 2	Total TRV
A	469.3	372.5	367.3	667.3
B	446.0	291.7	320.5	612.2
C	477.3	369.1	352.6	721.7

TABLE III CALCULATION RESULTS IN CASE OF 150 MVAR

Phase	Overvoltages on VSR U_{max} (kV)	TRV on circuit breaker U_{max} (kV)		
		Breaking chamber 1	Breaking chamber 2	Total TRV
A	387.7	322.3	354.3	676.6
B	429.3	302.6	334.1	636.7
C	463.3	393.9	365.0	761.6

Overvoltages on VSR (Fig. 25) were higher in case of 80 MVAR, while TRV on circuit breaker (Fig. 26) was higher in case of 150 MVAR. Highest TRV and overvoltages on VSR occurred in phase C which was firstly switched off. Surge arresters effectively limited both TRV on circuit breaker and overvoltages on VSR (Table IV).

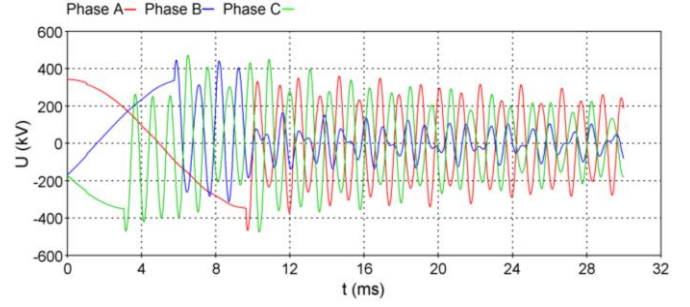


Fig. 25. Overvoltages on VSR (80 MVAR)

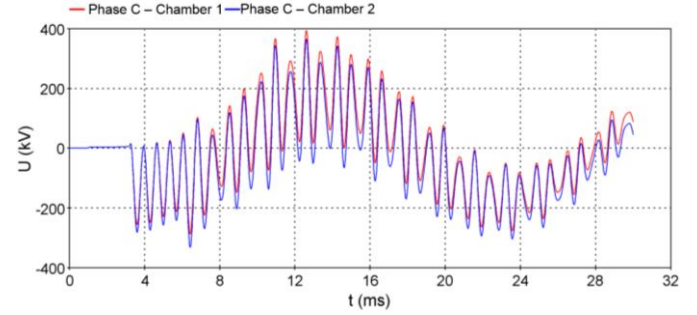


Fig. 26. TRV across breaking chambers in phase C (150 MVAR)

TABLE IV REDUCTION OF TRV AND OVERVOLTAGES ON VSR IN PHASE C DUE TO INSTALLATION OF SURGE ARRESTERS

	150 MVAR		80 MVAR	
	TRV (kV)	Overvoltages on VSR (kV)	TRV (kV)	Overvoltages on VSR (kV)
Without arresters	791.6	475.6	923.7	659.7
With arresters	761.6	463.3	721.7	477.3

VI. OVERVOLTAGES DUE TO ELECTRIC ARC REIGNITION

Reignition overvoltages are generated by the reignition following the initial interruption and arc extinction. Reignitions are provoked when the TRV across the circuit breaker contacts exceeds the dielectric strength (Fig. 27).

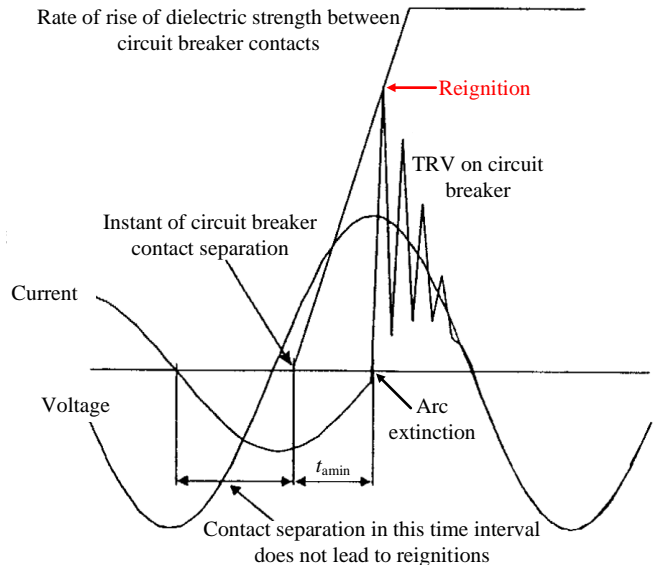


Fig. 27. Target for contact separation in order to eliminate reignitions

For arcing times shorter than t_{amin} , which represents the arcing time at which reignition is still probable, a high probability of reignition exists. Fig. 27 depicts two time instants of contact separation, with and without reignition.

Uncontrolled de-energization will, in a typical case, cause reignition in at least one circuit breaker pole. By controlling the contact separation in such a manner that arcing times shorter than t_{amin} will not occur, reignitions will be eliminated.

The occurrence of reignition depends of system configuration and circuit breaker performances. Reignition can be usually expected near the peak value of the TRV where the voltage difference across the circuit breaker is around 2 p.u.

Reignition in phase A at peak value of TRV is shown in Fig. 28 and overvoltages on VSR for 80 MVar in case without surge arresters are shown in Fig. 29.

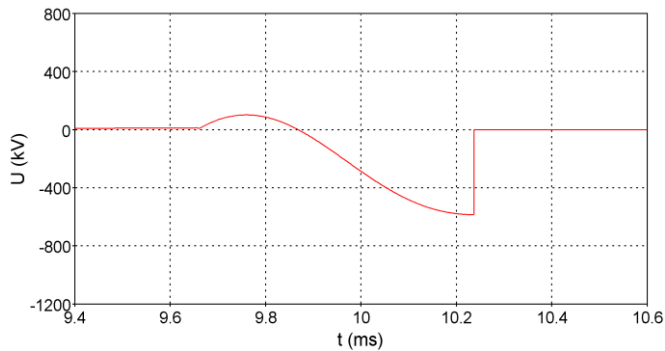


Fig. 28. TRV across circuit breaker in phase A

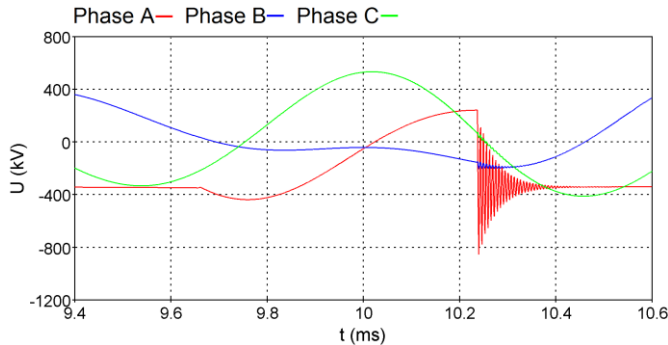


Fig. 29. Overvoltages on VSR due to reignition in phase A at peak value of the TRV

In this case, steepness of overvoltage in phase A was 376 kV/ μ s. Table V shows calculated overvoltages on VSR due to reignition at peak value of TRV in phase A.

TABLE V OVERVOLTAGES DUE TO ARC REIGNITION

	Overvoltages on VSR U_{max} (kV)	
	150 MVar	80 MVar
Without surge arresters	904.5	857.3
With surge arresters	677.8	673.1

Overvoltages caused by reignition were not critical considering insulation breakdown of VSR, as it was protected by surge arresters. However, steep wave front overvoltages

stress the insulation of the first few winding turns.

VII. CONCLUSIONS

This paper describes switching transients caused by uncontrolled and controlled switching of three-phase 420 kV variable shunt reactor (VSR) at tap positions corresponding to lowest (80 MVar) and highest (150 MVar) reactive power. EMTP-RV model was developed, which includes dynamic behavior of electric arc in SF₆ circuit breaker.

The simulations showed that inrush currents and zero-sequence currents were significantly lower in case of 80 MVar compared to 150 MVar. Therefore, the energization of VSR at 80 MVar is recommended. Controlled energization successfully reduced the amplitudes and DC components of inrush currents and zero-sequence current.

Overvoltages on VSR and transient recovery voltage on circuit breaker were calculated during VSR de-energization. The analysis showed that overvoltages were higher in case of 80 MVar. Therefore, de-energization of VSR at 150 MVar is recommended. MO surge arresters effectively limited both TRV on circuit breaker and overvoltages on VSR, which were lower than switching impulse withstand voltage (1050 kV, 250/2500 μ s).

Occurrence of reignition near the peak value of TRV was analyzed and reignition overvoltages were lower than lightning impulse withstand voltage (1425 kV, 1.2/50 μ s) of VSR. However, frequent exposure of VSR insulation to transients, especially steep reignition overvoltages, deteriorates its dielectric properties. In this particular case, calculated overvoltage steepness was lower than 772 kV/ μ s, recommended by [13].

The application of VSR controlled switching can completely eliminate the probability of circuit breaker reignition during de-energization.

VIII. REFERENCES

- [1] Z. Gajić, B. Hillstrom, F. Mekić, "HV shunt reactor secrets for protection engineers", 30th Western Protective Relaying Conference, Washington, 2003.
- [2] I. Uglešić, B. Filipović-Grčić, S. Bojić, "Transients Caused by Uncontrolled and Controlled Switching of Circuit Breakers", The International Symposium on High-Voltage Technique "Höfler's Days", 7-8 November 2013, Portorož, Slovenia.
- [3] I. Uglešić, S. Hutter, B. Filipović-Grčić, M. Krepela, F. Jakl, "Transients Due to Switching of 400 kV Shunt Reactor", International Conference on Power System Transients (IPST), Rio de Janeiro, Brazil, June 24-28, 2001.
- [4] Karcus M. C. Dantas, Washington L. A. Neves, Damásio Fernandes Jr., Gustavo A. Cardoso, Luiz C. Fonseca, "On Applying Controlled Switching to Transmission Lines: Case Studies", International Conference on Power Systems Transients (IPST), Kyoto, Japan June 3-6, 2009.
- [5] CIGRE TF13.00.1, "Controlled Switching, State-of-the-Art Survey", Part 1: ELECTRA, No.162, pp. 65-96, Part 2: Electra No.164, pp. 39-61, 1995.
- [6] Mitsubishi Electric Advance: "Controlled Switching System", vol.117, ISSN 1345-3041, Japan, 2007.
- [7] EMTP-RV, documentation, WEB site www.emtp.com.
- [8] J. Vernieri, B. Barbieri, P. Arnera, "Influence of the representation of the distribution transformer core configuration on voltages during

unbalanced operations”, International Conference on Power System Transients (IPST), Rio de Janeiro, 2001.

- [9] Ali F. Imece, D. W. Durbak, H. Elahi, S. Kolluri, A. Lux, D. Mader, T. E. McDemott, A. Morched, A. M. Mousa, R. Natarajan, L. Rugeles, and E. Tarasiewicz, "Modeling guidelines for fast front transients", Report prepared by the Fast Front Transients Task Force of the IEEE Modeling and Analysis of System Transients Working Group, *IEEE Transactions on Power Delivery*, Vol. 11, No. 1, January 1996.
- [10] CIGRE Technical brochure 135: "State of the art of circuit-breaker modeling", WG 13.01, 1998.
- [11] B. Filipović-Grčić, D. Filipović-Grčić, I. Uglešić, "Analysis of Transient Recovery Voltage in 400 kV SF₆ Circuit Breaker Due to Transmission Line Faults", *International Review of Electrical Engineering*, vol. 6, no. 5, Part B, pp. 2652-2658, 2011.
- [12] ABB, "Controlled Switching, Buyer's & Application Guide", Edition 4, 2013.
- [13] S. A. Morais, "Considerations on the Specification of Circuit-Breakers Intended to Interrupt Small Inductive Currents", *Electra*, no. 147, April 1993, pp. 45-69